A Continuum Description of Rarefied Gas Dynamics (III)— The Structures of Shock Waves

Xinzhong Chen
Astronomy Department, Columbia University, New York, NY 10027

Hongling Rao
Microeletronics Sciences Laboratories, Columbia University, New York, NY 10027

Edward A. Spiegel
Astronomy Department, Columbia University, New York, NY 10027

(Dated: February 1, 2008)

We use the one-dimensional steady version of the equations derived in paper I to compute the structure of shock waves. The agreement with experiment is good, especially when we retain the experimental value of the Prandtl number adopted in II.

I. INTRODUCTION

In the simplest descriptions of shock waves, one uses the Euler equations of fluid dynamics to develop jump conditions across the discontinuity that describes the shock. These conditions have qualitative value but there are problems for which such limiting solutions are not adequate. For example, in studying radiation from shock waves, say to infer the properties of the radiating atoms, the conditions within the shocks may become important. If the matter ahead of the shock is neutral and that behind the shock is fully ionized, the observed spectral lines may be formed in the shock itself and so conditions there need to be carefully worked out. This example is one of many that we might have cited to motivate our present study of the structure of shock waves. Even a cursory look at the literature on this problem gives a clear picture of the importance that has been attached to it.

Much of the work on the structure of shock waves has been aimed at improving on the description provided by the Navier-Stokes equations. A review of such attempts was given by Galkin *et. al.* [1], who compared various higher order solutions of Boltzmann equation with results from the Chapman-Enskog [3] and Hilbert methods [13]. In terms of shock structure alone, the higher order solutions give a significantly improved result [7, 8], but a number of fundamental problems concerning the status of these equations remain open [1, 9, 13, 14]. It is especially troubling that a large number of higher order nonlinear terms in some of the proposed improvements make it difficult to use the results in realistic problems. Similar difficulties beset extensions of Grad's moment method [13, 15], such as the Extended Irreversible Thermodynamics [16], which does give a good result for the problem of ultrasonic sound wave propagation. It remains true however, that a large number of equations must be solved to achieve a reasonable accuracy with EIT.

When the densities are sufficiently low, direct numerical simulation by the Monte Carlo method is the most reliable way to compute high-Knudsen-number flows, though the computational cost may be high in regimes near continuum limits [10]. A relatively new and effective method that has been described for direct solution of the relaxation (or BGKW) model does offer hope of improvement [11] but it remains to taken beyond the two-dimensional problems that it has so far tested very well on.

It thus appears that an effective macroscopic description would be of value for such problems and so, in this paper, we show how the equations derived in paper I may fill this need. To do this, we work out the structure of shock waves in one-dimensional steady flow starting from the equations of paper I. Those equations were derived from kinetic theory without using some of the traditional simplifications associated with the Chapman-Enskog approach. In particular, we did not use results from lower order approximations to simplify higher order equations. In paper II, the first-order development (in mean free path) of paper I was tested against observations of ultrasound propagation. We found good quantitative agreement between our theory and the experiments in the high Knudsen number regime where Navier-Stokes equations clearly fail. Though the success of our approach works well beyond the expected limits of validity of the theory, such occurrences are not unheard of in good asymptotic methods.

In the present paper, we go on to see how well the theory works for the computation of the structure of shock waves. Since the shock thickness is typically of the order of a mean free path, we again are pushing against the limits of validity of the expansions used in deriving the fluid equations. We confront in addition the added challenge of strong nonlinearity. Moerover the flow considered in shock theory can is far from thermodynamic equilibrium, so this too makes for a stringent test.

A simplification that makes the comparison relatively easy to draw is that, in the study of shocks, we may separate the continuum differential equations of fluid motion from the boundary conditions that must be stated to complete

a well-posed problem. The boundary conditions for the shock problem is not in question since we may impose the aforementioned jump conditions, expressed in terms of the Rankine-Hugoniot relations, to serve in the role of the boundary conditions. Hence in this study of shock structure, we are able to focus on effects due only to the differential equations themselves and so examine the validity of our version of the fluid equations.

In Sec. II, we recall the fluid dynamical equations derived in paper I. Then, in Sec. III, the structure of one-dimensional shock waves are computed and compared to analogous results obtained with the Navier-Stokes equations as well as with experiments. The paper concluded with a brief discussion in Sec. V.

II. STATEMENT OF THE EQUATIONS

In paper I we proposed a modification of the usual asymptotic techniques for deriving fluid equations from kinetic theory. Our procedure avoids the simplification introduced by Chapman and Enskog [3] in which the results of lower approximations are introduced into the higher approximations. When we proceed in this way, we obtain these fluid equations [4, 5, 6]:

$$\partial_t \rho + \nabla \cdot (\rho \mathbf{u}) = 0 \tag{2.1}$$

$$\partial_t \ u + \mathbf{u} \cdot \nabla \mathbf{u} + \frac{1}{\rho} \nabla \cdot \mathbb{P} = 0 \tag{2.2}$$

$$\partial_t T + \mathbf{u} \cdot \nabla T + \frac{2}{3\rho R} (\mathbb{P} : \nabla \mathbf{u} + \nabla \cdot \mathbf{Q}) = 0 \ , \tag{2.3}$$

where ρ is the mass density, $\mathbf{u}$ is the average velocity of the particles in a fluid element cell, and T is the temperature. We assume that the gas is made up of identical, structureless particles with mass m so that $R = k/m$ is the gas constant with k the Boltzmann constant. Our expression for the stress tensor is

$$\mathbb{P} = \left[\rho R T - \mu \frac{D \ln T}{Dt} + \frac{2}{3} \nabla \cdot \mathbf{u}) \right] \mathbb{I} - \mu \mathbb{E} : \nabla \nabla \mathbf{u} \tag{2.4}$$

where

$$\frac{D}{Dt} = \partial_t + \mathbf{u} \cdot \nabla \ , \tag{2.5}$$

and

$$\mu = \tau \rho R T \tag{2.6}$$

is the viscosity expressed in terms of the mean free time τ. For the stress tensor we found

$$E^{ij} = \frac{\partial u^i}{\partial x_j} + \frac{\partial u^j}{\partial x_i} - \frac{2}{3} \nabla \cdot \mathbf{u} \, \delta^{ij} \ . \tag{2.7}$$

and for the heat current, we have

$$\mathbf{Q} = -\eta \nabla \ln(\rho T^{-\frac{3}{2}}) - \frac{7}{2} \eta \nabla \ln T - \frac{5}{2} \mu \frac{D\mathbf{u}}{\mathbf{Dt}} \ , \tag{2.8}$$

where $\eta = \frac{5}{2} \mu R T$ for the relaxation model.

By contrast, in the Navier-Stokes equations with no bulk viscosity, one has

$$\mathbb{P} = \rho R T \mathbb{I} - \mu \mathbb{E} : \nabla \nabla \mathbf{u} \tag{2.9}$$

and

$$\mathbf{Q} = -\eta \nabla \ln T \ . \tag{2.10}$$

III. SHOCK THEORY

A. Basic equations

As inidcated in Fig. 1, when the velocity of the flow in the upstream ($x \to -\infty$) exceeds the sound speed of the medium, a shock front forms. In a frame comoving with the shock front, we see a steady shock layer, whose structure is determined by the upstream thermodynamic quantities and the dissipation mechanism. The structure of the shock wave provides a straightforward test of the equations.

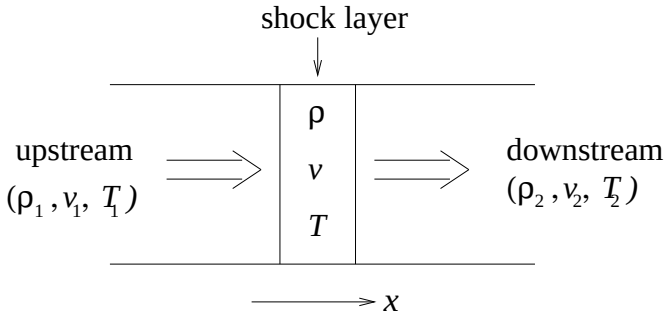

FIG. 1: The schematic diagram of a shock wave

Let us use subscripts 1 and 2 to denote values at large distances upstream ($x \to -\infty$) and downstream ($x \to \infty$) of the shock front, with $\mathbf{u} = (v(x), 0, 0)$, ρ and T as functions of only x. In the frame comoving with the shock front, we have $\partial_t = 0$. On integrating (2.1) to (2.3) from uniform upstream state to an arbitrary position x in the shock, we obtain

$$\rho v = \rho_1 v_1 \tag{3.1}$$

$$p + \rho v^2 + E^{11} = p_1 + \rho_1 v_1 \tag{3.2}$$

$$\rho v(c_v T + \frac{1}{2}v^2) + pv + v\pi_{xx} + q_x = \rho_1 v_1(c_v T_1 + \frac{1}{2}v_1^2) + p_1 v_1 \ , \tag{3.3}$$

where $c_v = \frac{3}{2}R$, E_{11} is the $\hat{x}\hat{x}$ component of the viscous stress tensor, and Q^1 is the $\hat{x}$ component of the heat current. The simple form of the right sides of these equations results from the vanishing of the derivatives of the fluid variables far from the shock.

From (3.1), we can express ρ in terms of v:

$$\rho = \frac{\rho_1 v_1}{v} \ . \tag{3.4}$$

Combination of (3.4) with (3.2) and (3.3) leads to

$$E^{11} = R\rho_1 v_1 \left(\frac{T_1}{v_1} - \frac{T}{v}\right) + \rho_1 v_1(v_1 - v) \tag{3.5}$$

$$q^1 = \frac{3}{2}R\rho_1 v_1(T_1 - T) + p_1(v_1 - v) + \frac{1}{2}\rho_1 v_1(v_1 - v)^2 \ . \tag{3.6}$$

We nondimensionlize these equations using v_1 as the unit of speed T_1 as unit of temperature and the mean free path λ_1 at upstream infinity as the unit of length. Then, we introduce the nondimensional quantities $X = x/\lambda_1$, $w(X) = v/v_1$, $\theta(X) = T/T_1$ and

$$\varpi(X) = \frac{E^{11}}{p_1} \qquad \text{and} \qquad q(X) = \frac{Q^1}{p_1 v_1} \ . \tag{3.7}$$

The equations become

$$\varpi = 1 - \frac{\theta}{w} + \frac{5}{3}M_1^2(1-w) \tag{3.8}$$

$$\frac{2q}{3} = 1 - \theta + \frac{2}{3}(1-w) + \frac{5}{9}M_1^2(1-w)^2 \ , \tag{3.9}$$

where the Mach number is

$$M_1 = \frac{v_1}{c_1} \qquad \text{with} \qquad c_1 = \sqrt{\gamma k T_1}$$

and $\gamma = 5/3$.

We see in from (2.6) that the viscosity is $\mu = \tau p$, where τ is the mean flight time of the particles. In turn, τ is the mean free path over the mean speed, which is the local speed of sound. Here, we adopt the simplest form of the relaxation model, namely that with constant τ. Then, we follow Gilbarg *et al.* [12] and take

$$\mu = \frac{\lambda_1 p_1}{\sqrt{2RT_1}} s \ , \tag{3.10}$$

where s is a parameter that is adjusted according to the nature of the constituent particles. For argon, $s = 0.816$ has often been used [3], but Kestin *et al.* [17] suggest that $s = 0.64$ is a better value for argon. We shall adopt the latter, more recent value in these computations. As to the conductivity, the relaxation model gives $\eta = \frac{5}{2}\mu RT$ but, when the Boltzmann collision term is used, we obtain a slightly different value in better agreement with experiment. As the difference results from the atomic model rather than to fluid dynamical issues, we shall adopt the formula $\eta = 15\mu RT/4$ to remove the effects of the inaccuracy of the atomic model.

To these formulae we adjoin the the closure relations (2.4) and (2.8) that may be rewritten in nondimensional form as

$$\varpi = -\sqrt{\frac{5}{6}} M_1 s \left[2w' + w\frac{\theta'}{\theta} \right] \tag{3.11}$$

$$q = -\frac{3}{2}\sqrt{\frac{5}{6}} \frac{s}{M_1} \left[2\theta' + \frac{10}{9} M_1^2 w w' - \theta \frac{w'}{w} \right] \ , \tag{3.12}$$

where the primes indicate differentiation with respect to X.

On combining (3.11) and (3.12) with (3.8) and (3.9), we obtain these equations:

$$-\sqrt{\frac{5}{6}} M_1 s \left[2w' + w\frac{\theta'}{\theta} \right] = 1 - \frac{\theta}{w} + \frac{5}{3}M_1^2(1-w) \tag{3.13}$$

$$-\frac{3}{2}\sqrt{\frac{5}{6}} \frac{s}{M_1} \left[2\theta' + \frac{10}{9} M_1^2 w w' - \theta \frac{w'}{w} \right] = 1 - \theta + \frac{2}{3}(1-w) + \frac{5}{9}M_1^2(1-w)^2 \ . \tag{3.14}$$

For comparison, we also write down the equations determining the shock structure from the Navier-Stokes equations:

$$-\frac{4}{3}\sqrt{\frac{5}{6}} M_1 s w' = 1 - \frac{\theta}{w} + \frac{5}{3}M_1^2(1-w) \tag{3.15}$$

$$-\frac{3}{2}\sqrt{\frac{5}{6}} \frac{s}{M_1} \theta' = 1 - \theta + \frac{2}{3}(1-w) + \frac{5}{9}M_1^2(1-w)^2 \ . \tag{3.16}$$

B. Critical Mach number

Before carrying out the numerical integration of equations (3.13)−(3.14), we examine them to draw some general conclusions. First, we observe that, since the x-derivatives of w and θ vanish far upstream and downstream, the right sides of equations (3.13)-(3.14) (as well as of (3.15)-(3.16)) must vanish there. These conditions provide two simultaneous equations which are readily solved for the fixed points $(w_1, \theta_1) = (1, 1)$ and

$$(w_2, \theta_2) = \left(\frac{M_1^2 + 3}{4M_1^2} \, \frac{5M_1^4 + 14M_1^2 - 3}{16M_1^2} \right) \ .$$

Our aim is to find solutions that connect the two fixed points. However, in the case of our equations, though the fixed points must occur at the locations just found in the (w, θ) plane, those locations need not be fixed points: the left sides of (3.13)-(3.14) may vanish when the determinant of the matrix of the coefficients of the derivatives vanishes. This is seen when we write the equations in the standard form

$$\mathcal{M}\begin{pmatrix} w' \\ \theta' \end{pmatrix} = -\frac{1}{s}\sqrt{\frac{6}{5}}\begin{pmatrix} \varpi/M_1 \\ M_1 q \end{pmatrix} \tag{3.17}$$

where

$$\mathcal{M} = \begin{pmatrix} 2 & w/\theta \\ \xi w - \theta/w & 2 \end{pmatrix} \tag{3.18}$$

with $\xi = 10M_1^2/9$.

If we can solve (3.17)-(3.18) to obtain explicit expressions for the derivatives, we can then solve the coupled first-order ordinary differential equations to find solutions connecting the fixed points. This is possible if the determinant of $\mathcal{M}$ does not vanish. The critical condition is then obtained by setting the determinant to zero, a step that leads to the relation

$$\theta = \frac{2}{9}M_1^2 w^2 \ . \tag{3.19}$$

At upstream infinity, we have $(w, \theta) = (1, 1)$ and this leads to the critical value $M_1 = 3/\sqrt{2} \approx 2.12$. We cannot solve for the derivatives when M_1 exceeds this value and so the theory breaks down above this value.

When the upstream flow speed is large enough to make the Mach number surpass the critical Mach number M_1^c, D changes its sign. If this leads to either $\frac{D_\omega}{D} > 0$ or $\frac{D_\theta}{D} < 0$ near the upstream, which is true for our case here, it will be impossible to match the downstream values monotonically. This happens for any hyperbolic system, as is commonly seen in moment formalisms [16] and first noticed in Grad's 13-moment method. Interestingly, it is numerically verified [16, 18] that only when the largest upstream critical Mach number is surpassed, does the above situation happen. As more and more moments are included, the largest critical Mach number becomes larger and larger, which in a sense partly relaxes the constraints on the application to shock study with moment method. It is thus expected that with the higher-order terms included in our formalism, the range of the Mach number will be extended. Nevertheless, the constraints on the Mach number is not due to the expansion scheme, but due to the nature of the relaxational model. In a following paper, we shall show that, when classical Boltzmann integral is used in place of the relaxation term, the constraints on Mach number will be removed. However, physically, information speed can not be infinite, which indicates that the final version of hydrodynamics must be of hyperbolic nature. Intuitively, this issue can only be addressed consistently under the frame of relativity. Amazingly, when our modified Hilbert expansion is applied to relativistic Boltzmann equation [6], a causal hydrodynamics which has constraints on the Mach number originated from relativity is obtained. Such a hydrodynamics is free of the stability problem and causality problem inherent in the Steward-Israel version of hydrodynamics [19, 20], the relativistic counterpart of N-S formalism. For our present purpose, we are content with the nonrelativistic version. The major concern here is whether the accuracy is improved when Knudsen number is not small.

C. Comparisons

We integrate the equations (3.13)∼(3.14) with different Mach number and make comparisons on the following aspects.

1. Shock profiles

In order to facilitate the comparison, let us first introduce quantities dP and dQ which are defined as the difference of stress and the heat current between the new version and the conventional N-S formalism. The definitions are the following:

$$\Delta\mathbb{P} = -\mu\left[\mathcal{D}_0 \ln T + \frac{2}{3}\nabla\cdot\mathbf{u}\right]\mathbb{I} \ , \tag{3.20}$$

$$\Delta\mathbf{Q} = -\left(\eta\nabla\ln(\rho T) + \frac{5}{2}\mu\mathcal{D}_0\mathbf{u}\right) \ . \tag{3.21}$$

For one-D flow, we obtain

$$\Delta\mathbf{P} = \Delta P\hat{x}\hat{x} \ , \tag{3.22}$$

$$\Delta\mathbf{Q} = \Delta Q\hat{x} \tag{3.23}$$

with ΔP and ΔQ given by

$$\Delta P = -\mu\left(\mathcal{D}_0\ln T + \frac{2}{3}v'\right) \ , \tag{3.24}$$

$$\Delta Q = -\left\{\eta[\ln(\rho T)]' + \frac{5}{2}\mathcal{D}_0 v\right\} \ . \tag{3.25}$$

In the study of shock wave, the upstream quantities are used to rewrite the aforementioned dimensionless dP and dQ:

$$dP \equiv \frac{\Delta P}{p_1} = -\sqrt{\frac{\gamma}{2}}sM_1\left(\frac{\theta'}{\theta} + \frac{2}{3}\omega'\right) \tag{3.26}$$

$$dQ \equiv \frac{2\Delta Q}{3p_1v_1} = -\frac{2}{3}\sqrt{\frac{\gamma}{2}}sM_1\left[\frac{15\theta}{4\gamma M_1^2}(\frac{\omega}{\omega'} - \frac{\theta'}{\theta} + \frac{5}{2}\omega\omega'\right] \ . \tag{3.27}$$

From the above definitions, we see that dP is equivalent to the bulk viscous pressure and dQ accounts for the extra heat current due to the non-adiabatic effect, both of which are taken as zero in the derivation of N-S formalism. Such an approximation is not justified when Knudsen number is not small, as will be shown in the following.

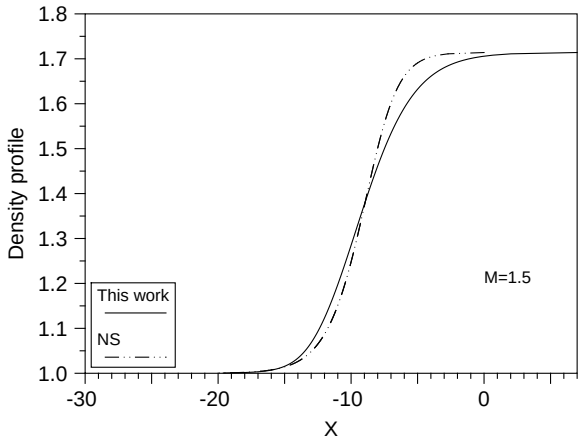

FIG. 2: Density profiles with Mach number M=1.5

Figures 2∼4 show the density, velocity and temperature profiles with $M_1 = 1.5$. It is seen that the profiles with the modified hydrodynamics are wider than those with N-S formalism. Such a trend is a well-known fact and has been verified experimentally.

The difference in the profiles are due to the nonzero dP and dQ, plotted in Fig. 5 and Fig. 6, respectively. A simple estimation shows that the dissipation due to these two extra effects increases monotonically from the downstream to the upstream, which tends to lower the gradients of the thermodynamical variables and results in a wider shock. Such effects become more noticeable when Mach number is larger, as is shown in Figs. 7∼11, where the same quantities as those in Figs. 2∼6 are plotted but with $M_1 = 2$. Compared to the case with $M_1 = 1.5$, the profiles are steeper and more asymmetric. The difference of the two versions of hydrodynamics is now more significant due to the increase in the Knudsen number with the Mach number. From Figs. 10∼ 11, it is clear that the bulk viscous pressure and the non-adiabatic heat current are no longer negligible.

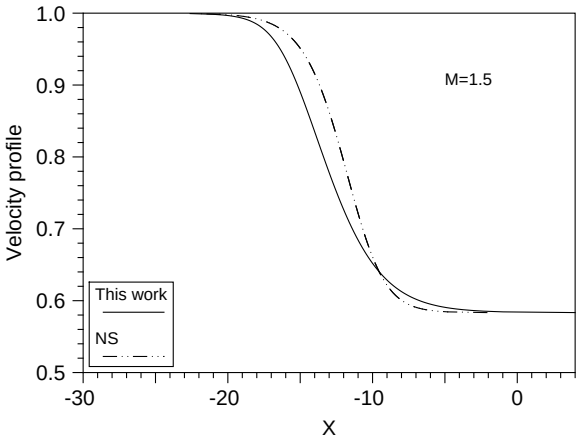

FIG. 3: Velocity profiles with Mach number M=1.5

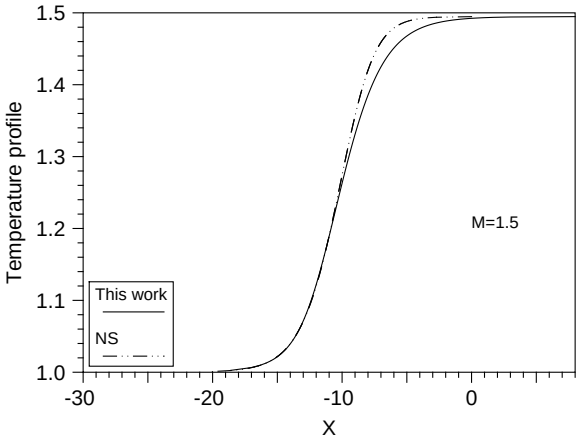

FIG. 4: Temperature profiles with Mach number M=1.5

2. Inverse thickness, asymmetry and T-ρ separation

The inverse thickness is defined as

$$\delta^{-1} = \frac{\rho'_m}{\rho_2 - \rho_1} \ , \tag{3.28}$$

where ρ'_m is the maximum value of the gradient of density profile, and as before ρ_1 and ρ_2 are the upstream and downstream values, respectively.

The asymmetry parameter [8] is defined as

$$A_s = \frac{\int_{\rho_a}^{\rho_2} \rho dx}{\int_{\rho_1}^{\rho_a} \rho dx} \tag{3.29}$$

with $\rho_a = \frac{1}{2}(\rho_2 - \rho_1)$.

Finally, the temperature-density separation $\Delta_{\rho T}$ is defined as the distance between the medium value points of temperature and density.

Figure 12 shows the inverse thickness versus Mach number. The experimental data for Argon and Xeron are also shown. Concluded from the plot, the modified hydrodynamics results in a wider shock for a given Mach number. In comparison with the experimental data and the direct Monte Carlo simulation results(for full Boltzmann equation),

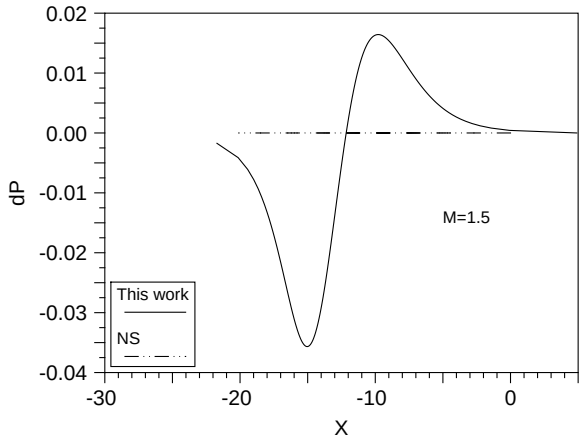

FIG. 5: dP profiles with Mach number M=1.5

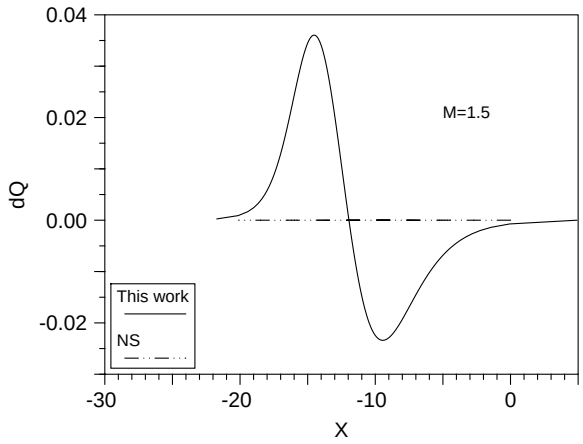

FIG. 6: dQ profiles with Mach number M=1.5

the accuracy is significantly improved. The physical explanation for the wider shock is as follows. The process-dependent bulk viscosity causes extra dissipation, which, combined with the non-adiabatic effect, makes the gradients of thermodynamic variables smoother and thus widens the shock.

As for the asymmetry parameter, in the case of $M_1 = 2.0$, N-S formalism gives $A_s = 1.25$, the modified one gives $A_s = 0.83$, which is closer to the experimental data 0.93. Aside from the quantitative improvement, the modified version also becomes qualitatively consistent with the experiment, i.e. A_s should be smaller than unity.

For the same Mach number $M_1 = 2.0$, N-S leads to a temperature-density separation of 1.04, whereas the modified version leads to 1.67 and the experimental data for Argon is 1.50 [8].

IV. CONCLUSIONS AND DISCUSSIONS

We have showed that the modified Hilbert expansion leads to a hydrodynamics of higher accuracy than that from the classic Chapman-Enskog expansion. In the study of rapid variation such as high-frequency sound wave propagation, this modified hydrodynamics provides a result consistent with experiment. The fitting is uniformly good for all range of Knudsen number. For the study of shock wave structures, within the range of its critical Mach number, it provides results comparable to those from direct Monte Carlo simulation. The physics underlying the new expansion scheme is that it relaxes the requirement that the gradient terms be small as is the case in CEE. This makes the method capable of deriving macroscopic equations valid for processes far from equilibrium. As we have seen in the shock structure study, the extra dissipation caused by the new mechanism of gradient of density smoothes the density profile. Such

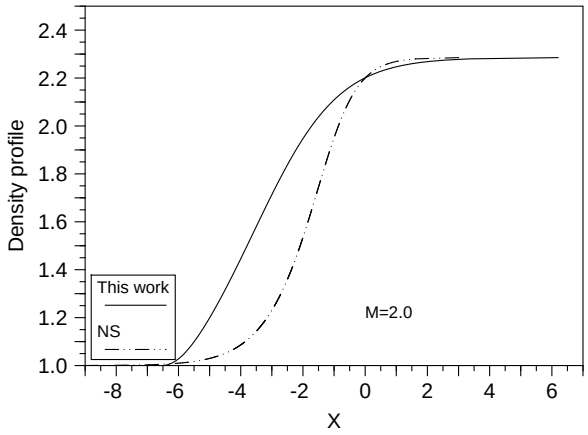

FIG. 7: Density profiles with Mach number M=2.0

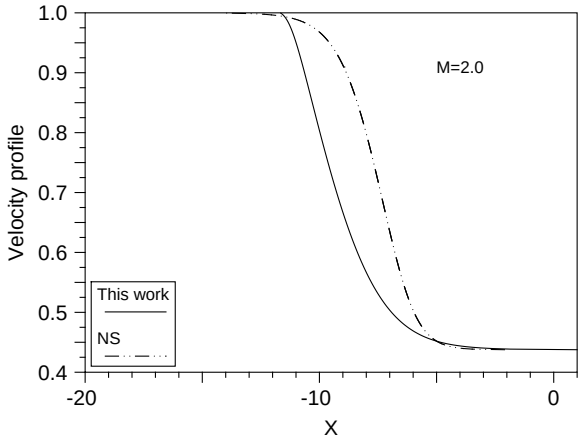

FIG. 8: Velocity profiles with Mach number M=2.0

a non-adiabatic dissipation is omitted in the Navier-Stokes formalism due to the extra constraints enforced by the CEE procedure in the derivation. As is discussed in section III, the existence of the critical Mach number is caused by the relaxation model we adopted for the kinetic equation. In one of our following papers [26] we will show that, when the Boltzmann collisional integral is used in place of the relaxation term, such a constraint on Mach number is removed. However, a consistent hydrodynamics satisfying causality principle yet without extra constraint beyond relativity on the possible Mach number can only be formulated with the relativistic Boltzmann equation, as will be shown in Ref. [27].

[1] V. Galkin and S. Shavaliev, Fluid Dynamics **33**, 469 (1998).
[2] O. Buzykin, V. Galkin, and V. Nosik, Fluid Dynamics **33**, 433 (1998).
[3] S. Chapman and T. G. Cowling, *The Mathematical Theory of Non-uniform Gases*, 3rd ed. (Cambridege University Press, Cambridge, 1970).
[4] X. Chen, Ph.D. thesis, Columbia University, 2000.
[5] X. Chen, H. Rao and E. A. Spiegel, Phys. Lett. A **271** 87 (2000).
[6] X. Chen, H. Rao and E.A. Spiegel, paper I.
[7] R. M. X. Zhong and R. Chapman, AIAA J. **31**, 1036 (1993).
[8] D. C. K. Fisko, in *Progress in Astronautics and Aeronautics, AIAA*, edited by D. W. E. Montz and D. Campbell (PUBLISHER, ADDRESS, 1989), Vol. 118.

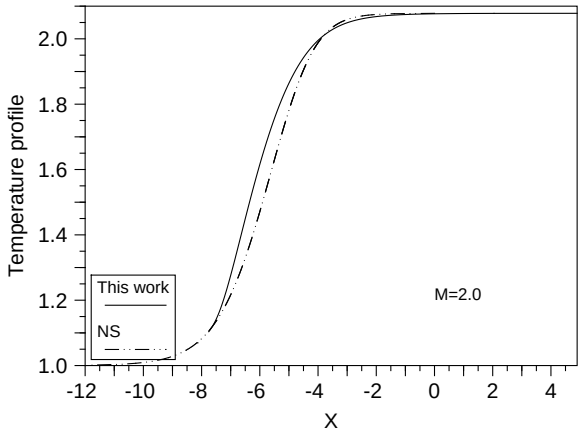

FIG. 9: Temperature profiles with Mach number M=2.0

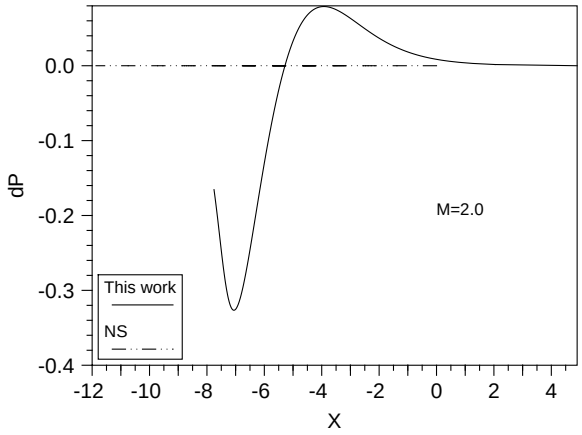

FIG. 10: dP profiles with Mach number M=2.0

[9] L. C. Woods, *An Introduction to Kinetic Theory of Gases and Magnetoplasma* (Oxford Univ. Press, ADDRESS, 1993).
[10] R. Myong, Physics of Fluids **11**, 2788 (1999).
[11] K. H. Prendergast and K. Xu, J. Comput. Phys. **109**, 53 (1993).
[12] D. Gilbarg and D. Paolucci, J. Rat. Mech. Anal. **2**, (1953).
[13] H. Grad, The Physics of Fluids **6(2)**, 147 (1963).
[14] Y. L. Klimontovich, Teoreticheskaya i Matematicheskaya Fizika **92(2)**, 909 (1992).
[15] H. Grad, Comm. Pure and App. Math. **2**, 331 (1949).
[16] I. Müller and T. Ruggeri, *Rational Extended Thermodynamics*, Vol. 37 of *Springer Tracts in Natural Philosophy*, 2nd ed. (Sprinter-Verlag, New York, 1998).
[17] J. Kestin *et al.*, J. Phys. Chem. Ref. Data **13**, (1984).
[18] W. Weiss, Phys. Review E, Part A **52**, (1995).
[19] J. Stewart, Proc. Roy. Soc. London **A 357**, 43 (1977).
[20] W. Israel and M. Stewart, Proc. Roy. Soc. London Ser. **A 365**, 43 (1979).
[21] M. Greenspan, J. acoust. Soc. Am. **28**, 644 (1956).
[22] G. S. E. Meyer, Zeitschr. f. Physik **149**, (1957).
[23] L. Sirovich and J. Thurber, J. Acoust. Soc. Am. **37**, 329 (1965).
[24] L. Sirovich and J. Thurber, J. Acoust. Soc. Am. **38**, 478 (1966).
[25] C. Cercignani, *The Boltzmann equation and its applications* (Springer-Verlag, New York, 1988).
[26] X. Chen, in preparation.
[27] X. Chen, in preparation.

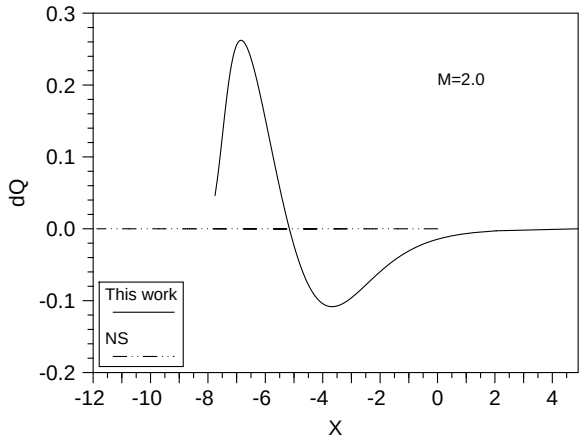

FIG. 11: dQ profiles with Mach number M=2.0

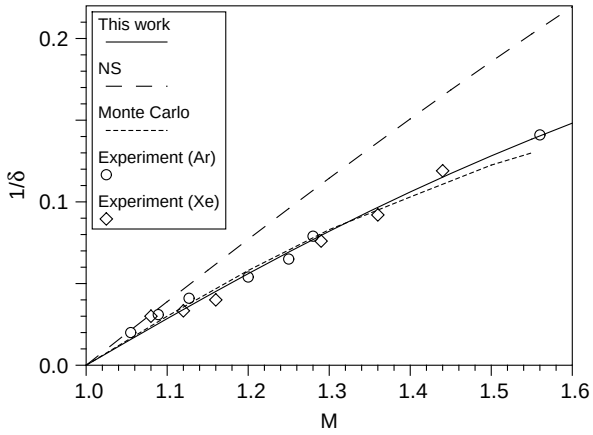

FIG. 12: Inverse density thickness